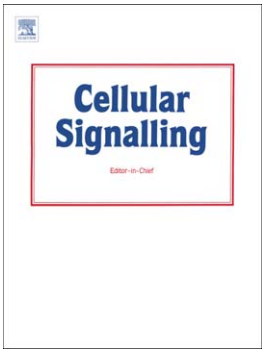

Cell confluence induces switching from proliferation to migratory signaling by site-selective phosphorylation of PDGF receptors on lipid raft platforms

Árpád Szöőr, László Ujlaky-Nagy, Gábor Tóth, János Szöllősi, György Vereb

PII: S0898-6568(15)30003-6
DOI: doi: 10.1016/j.cellsig.2015.11.012
Reference: CLS 8589

To appear in: *Cellular Signalling*

Received date: 29 June 2015
Revised date: 25 November 2015
Accepted date: 25 November 2015

Please cite this article as: Árpád Szöőr, László Ujlaky-Nagy, Gábor Tóth, János Szöllősi, György Vereb, Cell confluence induces switching from proliferation to migratory signaling by site-selective phosphorylation of PDGF receptors on lipid raft platforms, *Cellular Signalling* (2015), doi: 10.1016/j.cellsig.2015.11.012

Cell confluence induces switching from proliferation to migratory signaling by site-selective phosphorylation of PDGF receptors on lipid raft platforms

Árpád Szöőr[1], László Ujlaky-Nagy[2], Gábor Tóth[1], János Szöllősi[1,2] and György Vereb[1,2]

[1]Department of Biophysics and Cell Biology, and [2]MTA-DE Cell Biology and Signaling Research Group, Faculty of Medicine, University of Debrecen, Debrecen, Hungary

Running title: Cell confluence induced migratory signaling by site-selective phosphorylation

Address correspondence to: György Vereb, MD PhD, Department of Biophysics and Cell Biology, Faculty of Medicine, University of Debrecen, Egyetem tér 1, H-4032 Debrecen, Hungary. E-mail: vereb@med.unideb.hu

Abstract

Platelet derived growth factor receptors (PDGFR) play an important role in tumor pathogenesis and are frequently overexpressed in glioblastoma. Earlier we have shown that only confluent glioblastoma cell cultures exhibit a biphasic calcium transient upon PDGF stimulation. Here, we examined how the change in cell density leads to differential cellular responses to the same PDGF stimulus.

PDGF beta receptors and their specific phosphotyrosine residues were fluorescently co-labeled on A172 and T98G glioblastoma cells. The distribution in cell membrane microdomains (lipid rafts) and the phosphorylation state of PDGFR was measured by confocal microscopy and quantitated by digital image processing. Corresponding bulk data were obtained by Western blotting. Activation of relevant downstream signaling pathways was assessed by immunofluorescence in confocal microscopy and by Western blot analysis. Functional outcomes were confirmed with bulk and single cell proliferation assays and motility measurements.

In non-confluent (sparse) cultures PDGF-BB stimulation significantly increased phosphorylation of tyr716 specific for the Ras/MAPK pathway and tyr751 specific for the phosphoinositide 3-kinase/Akt pathway. As cell monolayers reached confluence, tyr771 and tyr1021 were the prominently phosphorylated residues. Tyr771 serves as adaptor for Ras-GAP, which inactivates the MAPK pathway, and tyr1021 feeds into the phospholipase C-gamma / PKC pathway. Coherent with this, MAPK phosphorylation, Ki67 positivity and proliferation dominated in dispersed cells, and could be abolished with inhibitors of the MAPK pathway. At the same time, RhoA activation, redistribution of cortactin to leading edges, and increased motility were the prominent output features in confluent cultures. Importantly, the stimulus-evoked confluence-specific changes in the phosphorylation of tyrosine residues occurred mainly in GM1-rich lipid microdomains (rafts).

These observations suggest that the same stimulus is able to promote distinctly relevant signaling outputs through a confluence dependent, lipid raft-based regulatory mechanism. In particular, cell division and survival in sparse cultures and inhibition of proliferation and promotion of migration in confluent monolayers. In our model, the ability to switch the final output of the same stimulus as a function of cell density could be a key to the balance of proliferation and invasion in malignant glioblastoma.

Key words: lipid rafts, site-selective phosphorylation, quantitative confocal microscopy, contact inhibition, tumor proliferation, invasive tumor growth, cell migration, glioblastoma, PDGFR

Abbreviations

DAG	diacylglycerol
GM1	monosialotetrahexosylganglioside
GRB2	growth factor receptor binding protein-2
IP3	inositol 1,4,5-trisphosphate
PDGF	platelet-derived growth factor
PDGF-BB	homodimer of the B isoform of platelet derived growth factor)
PDGFR	platelet-derived growth factor receptor
PI3-kinase	phosphatidylinositide 3′-kinase
PKC	protein kinase C
PLCγ	phospholipase C-γ1
PtdIns(3,4,5)-P3	phosphatidylinositol (3,4,5)-trisphosphate
PTPN1	protein tyrosine phosphatase, non-receptor, type 1 (PTP1B)
Ras-GAP	GTPase activator of Ras
Ras-MAPK	Ras mediated mitogen-activated protein kinase
SH2 domain	Src Homology 2 domain
Tyr716	tyrosine residue 716
Tyr751	tyrosine residue 751
Tyr771	tyrosine residue 771
Tyr1021	tyrosine residue 1021

1. **Introduction**

Platelet-derived growth factors (PDGFs) and their receptors (PDGFRs) have been demonstrated as prototypes for growth factor and receptor tyrosine kinase function for more than 30 years. PDGF stimulates migration and proliferation of connective tissue cells and has an important role during embryonic development and wound healing [1], but its abnormal expression also contributes to a variety of diseases [2]. PDGF and its receptor are currently under investigation as targets in numerous proliferative disorders, including cancers, fibrosis, and cardiovascular diseases [2]. PDGFR-β plays an important role in the regulation of human malignant gliomas [3, 4]. PDGF and PDGFR expression correlates with tumor grade and proliferative activity [5-7], and inhibition of PDGFR-β drastically reduces the proliferation and migration of glioblastoma cells [8].

Phosphotyrosine residues on the activated PDGFR initiate downstream signaling. On PDGFR- β, tyrosine 716 (Tyr716) is an important residue which binds the growth factor receptor binding protein-2 (GRB2). This SH2 domain protein activates the Ras-MAPK pathway [9] which plays a central role in cell proliferation. Dephosphorylation of Tyr716 by protein tyrosine phosphatase PTPN1 (PTP1B) inhibits PDGF-induced ERK1/2 MAPK activation [10]. The negative regulation of this pathway is mediated by the phosphorylation of tyrosine 771 (Tyr771) leading to the binding of Ras-GAP, the GTPase activator of Ras [11]. Phosphorylation of Tyr771 is regulated by protein tyrosine phosphatase PTPN11 (SHP-2) [12]. Dephosphorylation of Tyr771 decreases the recruitment of Ras-GAP leading to prolonged activation of the Ras/MAP kinase pathway and thus promoting cell proliferation.

Tyrosine 751 (Tyr751) is situated in the kinase insert region and binds the regulatory p85 subunit of phosphatidylinositide 3′-kinase (PI3-kinase) [13]. The phosphatidylinositol (3,4,5)-trisphosphate (PtdIns(3,4,5)-P3) generated by PI3-kinase enhances the activity of the pro-survival Akt kinase [14, 15]. PTPN1 is also able to dephosphorylate Tyr751 on PDGFR, thus decreasing activation of Akt [10].

Tyrosine 1021 (Tyr1021) is known as the binding site of phospholipase C-γ1 (PLCγ) [16]. PLCγ initiates the inositol 1,4,5-trisphosphate (Ins (1,4,5)-P3) / diacylglycerol (DAG) pathway, which mediates intracellular calcium mobilization and protein kinase C (PKC) activation [17] and is important in the regulation of cell migration [16, 18].

GM1 rich microdomains (lipid rafts) of the cell membrane play crucial role in growth factor induced signal transduction [19, 20]. These plasma membrane microdomains enriched in cholesterol and sphingolipids are able to segregate cellular processes during signal transduction by promoting isolated assembly of membrane protein superstructures [21] and to focus signaling input by accumulation of specific receptors [22, 23].

Under normal conditions, cell growth and motility are regulated not only by the availability of growth factors but also by a number of positive and negative co-stimuli delivered by the extracellular matrix and the neighboring cells. Increasing number of cell–cell contacts leads to an arrest of proliferation known as contact inhibition [24]. When normal cells undergo malignant transformation, they can lose contact inhibition causing abnormal cell proliferation and migration [25]. In the case of PDGFR mediated cell proliferation, contact inhibition correlates with low molecular weight phosphotyrosine phosphatase mediated dephosphorylation of the receptor [26].

Previously we have shown that PDGF stimulated glioblastoma cells respond with prolonged biphasic rises of intracellular free calcium concentration when cultures were confluent, however, in sparse cultures this response largely disappears [27]. The distinct behavior was independent of cell cycle [27], however, preliminary experiments hinted that PDGFR expression and lipid raft localization did change with cell culture confluence. Consequently, in the present study we examined how segregation of PDGFR by GM1 rich microdomains could regulate a differential cellular response as a function of cell confluence in glioblastoma cells. We have found that even though the same receptors are stimulated by the same ligand, tyrosine residues that initiate distinct pathways are selectively phosphorylated in lipid rafts and stimulate functions inherently appropriate for the status of tumor cells: sparse cells enter the mitotic cycle, whereas confluent cells start to migrate.

2. Materials and methods

All materials were from Sigma-Aldrich (St. Louis, MO) unless otherwise indicated.

2.1. Cell Culture

A172 (CRL-1620) and T98G (CRL-1690) human glioblastoma cells obtained from American Type Culture Collection were maintained in a humidified incubator at 37°C in a 5% CO_2

atmosphere in Dulbecco's Minimal Essential Medium supplemented with 10% fetal calf serum and antibiotics. Cells were passaged three times a week.

For confocal microscopy, cells were seeded onto 12 mm glass coverslips (0.17 mm, Menzel-Glaser, Braunschweig, Germany) at various densities. We used sparse/low density and confluent/high density cell cultures. Initial cell concentration was 15,000/cm^2 for sparse and 60,000/cm^2 for confluent conditions. Cells were cultured for 2 days before measurements, unless otherwise stated.

For Western blot experiments, cells were seeded onto cell culture dishes (Corning, via Sigma-Aldrich). Sparse/low density and confluent/high density cultures were used. 570,000 cells were seeded in 100 mm and 35 mm petri dishes which meant 7,250 and 60,000 cells/cm^2 for sparse and confluent samples, respectively. Cells were cultured for 2 days before measurements.

Before experiments, cells were starved in serum-free HEPES buffer, pH: 7.4, for 2h at 37°C. Ligand stimulation of PDGFR-β was done with the recombinant homodimer of the B isoform of platelet derived growth factor (PDGF-BB) at 37°C. PDGF-BB was used at a final concentration of 20 ng/ml, the lowest dose previously established to cause maximum calcium signals in confluent glioblastoma cell cultures [28]. For microscopy experiments, ligand stimulation was 2 minutes long when measuring receptor phosphorylation, and 2 hours when assessing migration and proliferation. In order to determine the time-dependence of the events, PDGF-BB stimulation was performed for 1, 2, 5, 15, 30 and 60 minutes for Western blot-based analysis of signaling.

2.2. Immunofluorescent labeling

Cells on coverslips were washed three times in ice-cold HEPES buffer and incubated with anti-PDGFR-β mAb (10 μg/ml, RD Systems PR7212) for 10 minutes on ice. After three washes, Cy3-conjugated secondary goat anti-mouse Fab antibody (Jackson ImmunoResearch Europe Ltd., Suffolk, UK) was added at 15 μg/ml together with 4 μg/ml Alexa Fluor 488-conjugated cholera toxin B-subunit (Invitrogene / Life Technologies, Carlsbad. CA) for 10 min on ice. The cholera toxin B-subunit binds to monosialotetrahexosylganglioside (GM1) glycosphingolipid rich domains and serves as one of the most widely used markers of lipid rafts. After three washes (1, 3 and 5 min), cells were prefixed with 1% paraformaldehyde for 10 minutes on ice, then the cell membrane was permeabilized with HEPES buffer containing 0.1% Triton-X 100 and 1% BSA for 10 minutes. Phosphotyrosine 716, 751, 771 and 1021 residues of PDGFR were labeled with indirect immunofluorescence. Following incubation

with the appropriate mAb (sc-16569-R, sc-21902-R, sc-17174-R, sc-12909-R respectively, Santa Cruz Biotechnologies, Dallas, TX, 12 μg/ml final concentration) for 35 minutes at RT, cells were washed three times (for 2, 4 and 5 minutes) with HEPES buffer containing 0.05% Triton-X 100. Primary antibodies were labeled with Alexa Fluor 647 conjugated secondary goat-anti-rabbit antibody (20 min, RT, 10 μg/ml, Invitrogen / Life Technologies, Carlsbad. CA). After three washes, cells were fixed with 4% freshly depolymerized paraformaldehyde. Finally, the coverslips were mounted with Mowiol. Negative controls with one of the primary antibodies omitted, as well as with single secondary antibodies and with no labeling at all were also prepared and confirmed to lack signal in the appropriate fluorescence channel.

For microscopic assessment of cell proliferation and cell migration, intracellular indirect labeling was performed using the same protocol as above, starting with washing, fixation and permeabilization. Primary antibodies were used at 4 μg/ml (M7240 against Ki67 from Dako, Glostrup, Denmark, and 05-180 antibody against cortactin from Merck Millipore, Darmstadt, Germany) or at 8 μg/ml (sc-32954 against p(Ser188)RhoA from Santa Cruz Biotechnologies, Dallas, TX). Secondary goat anti-mouse (against M7240 and 05-180) and goat anti-rabbit (against sc-32954) antibodies from Invitrogen / Life Technologies were either Alexa Fluor 647 or Alexa Fluor 546 conjugated and used at 10 μg/ml final concentration.

2.3. Confocal Laser Scanning Microscopy

Membrane distribution of PDGFR-β and its phosphotyrosine residues was quantitatively analyzed by a confocal laser scanning microscope (LSM 510, Carl Zeiss GmbH, Jena, Germany). Alexa Fluor 488 was excited at 488 nm, Cy3 and Alexa Fluor 546 at 543 nm, and Alexa Fluor 647 at 633 nm. Their fluorescence emission was detected through 505 to 550-nm, 560 to 615 band-pass and 650-nm long-pass filters, respectively. The images were taken in multitrack mode to completely exclude channel cross talk. 512 × 512-pixel, 1.5 μm thick optical sections were obtained with a 40× C-Apochromat water immersion objective (NA=1.2).

2.4. Determining colocalization from image cross-correlation

Colocalization of any two molecules at the few-hundred-nanometer scale was determined from confocal laser scanning microscopy images of double-labeled cells. The optical section was taken from the top horizontal slice of the membrane of adherent cells (Figure 1A). The images were gated on the presence (above-background intensity) of at least one of the

fluorophores. For a pair of images, x and y, the cross-correlation coefficient C of the two labels was calculated as:

$$C = \frac{\sum_i \sum_j (x_{i,j} - \bar{x})(y_{i,j} - \bar{y})}{\sqrt{\sum_i \sum_j (x_{i,j} - \bar{x})^2 \sum_i \sum_j (y_{i,j} - \bar{y})^2}}$$

where x_{ij} and y_{ij} are fluorescence intensities at pixel coordinates i, j in images x and y and $\bar{x}$ and $\bar{y}$ designate the mean intensities in each channel. The theoretical maximum is C = 1 for identical images and a value close to 0 implies independent random localization of the labeled molecules. A custom program written in LabView was used to analyze the images [23]. The average intensity of labels in the membrane was also evaluated by the program.

2.5. Digital image processing for quantitative analysis of specific phosphotyrosine distribution inside and outside of lipid rafts

A quantitative digital image processing pipeline, created for this purpose in ImageJ [29], was used to calculate specific phosphotyrosine density inside and outside of lipid rafts. First, background intensities of phosphotyrosine and GM1 positive channels were subtracted. Two binary masks in inverse relation – raft and non-raft – were created and used to generate inside raft and outside raft phosphotyrosine images. From these, probability distribution curves of pixel-intensities were generated, and the mean intensities calculated (see Figure 1B-F).

2.6. Digital image processing for quantitative analysis of specific relative receptor phosphorylation inside and outside of lipid rafts

The ImageJ algorithm developed for this purpose starts by subtracting the background in the PDGFR, phosphotyrosine and GM1 channels, and then normalizes the intensity of the specific phosphotyrosine label to the total PDGFR on a pixel by pixel basis. The image generated this way represents the relative specific PDGFR phosphorylation on the cell surface. Raft and non-raft binary mask are then created from the GM1 channel and applied to calculate the mean relative receptor phosphorylation inside and outside of lipid rafts. Finally, the inside raft value is normalized to the outside raft value, so that acquisition parameters that could change across experiments are canceled and allow the pooled evaluation of results from many independent experiments (Figure 2A). Values of the final quotient above and below 1 indicate

preferential phosphorylation and dephosphorylation, respectively, of a given tyrosine residue inside rafts (Figure 2C-F).

2.7. Western blotting

Cells were washed with ice cold HEPES buffer and lysed with RD lysis buffer containing 20mM Tris, 0.1% NP40, 137 mM NaCl, 10% glycerol, 2mM EDTA, 2mM PMSF, 1mM Na-ortho-vanadate, and Protease Inhibitory Cocktail, (ROCHE, according to the manufacturer's instructions). Protein concentration was measured according to Bradford, samples were diluted with SDS-PAGE sample buffer to contain the same concentration of total protein and finally boiled for 10 min. Proteins (20 µg per well) were separated by 6-12% SDS-PAGE gels depending on the targeted molar mass, and electrophoretically transferred to polyvinylidene difluoride membranes (Merck Millipore, Darmstadt, Germany). The same antibodies against phosphotyrosine-residues 716, 751, 771, 1021, and pRhoA as for microscopy were used at 0.5 µg/ml. pP38 MAP kinase, pP42/44 MAP Kinase, and pAkt were detected with the following antibodies: 9211S (0.3 µg/ml, Cell Signaling Technology, Danvers, MA), 9106S (0.3 µg/ml, Cell Signaling), and 05-669 (0.7 µg/ml, Merck Millipore, Darmstadt, Germany). Total cellular protein was controlled by detecting actin with antibody A3853 (0.1 µg/ml, Sigma-Aldrich, St. Louis, MO). After overnight incubation on a rocking table at 4°C, membranes were washed with TBS-T (50 mM Tris, 150 mM NaCl, 0.1% Tween 20) for 30 minutes at room temperature, then peroxidase-conjugated secondary goat anti-mouse (A4416) or goat anti-rabbit (A0545) antibody (1 µg/ml, Sigma-Aldrich, St. Louis, MO) was added for 2 hours. After a 30-minute wash with TBS-T, membranes were developed with Super Signal West Pico Chemiluminescent Substrate (Thermo Fischer Scientific, Waltham, MA) for 2 minutes and imaged with a FluorChem Q system (ProteinSimple, San Jose, CA).

2.8. Assessment of cell proliferation

Proliferation in confluent and sparse cultures was measured using an MTT based colorimetric assay (EZ4U, Biomedica GmbH, Wien, Austria). Cells plated at various densities (9,000 through 150,000/cm^2) were grown in 96-well plates for 2 days. After incubation with EZ4U, a Synergy HT Multi-Detection microplate Reader (Bio-Tek, Winooski, VT) was used to measure 488 nm absorption, which was corrected with the 620 nm absorption and then converted to cell numbers using a calibration curve prepared using parallel measurements of freshly plated and adhered cells seeded at various densities. Cell numbers were averaged

(n=6), and growth was expressed as a multiple of initial cell number, and plotted as a function of initial cell density.

To follow the growth rate continuously, real time cell adherence assay (RTCA) based on impedance measurement was performed using an ECIS ZΘ analyzer (Applied Biophysics, Troy, NY). T98G cells were grown in 8W10E PET 8-well arrays with gold electrodes at the bottom, seeded at low (15,000/cm^2) and high (60,000/cm^2) densities. Weak alternating current was applied at frequencies from 1 to 100,000Hz to continuously measure the complex impedance spectrum of cells adhering to each electrode in the well. The measured impedance at any time point is proportional to the area of the electrode covered by cells. Impedance values from 4 wells were averaged, normalized to initial cell number, and plotted as a function of time.

For testing the antiproliferative effect of various MAPK pathway inhibitors, we have used live cell imaging followed by cell counting, so that mitotic events could be visually verified. This way the possible metabolic effects of the inhibitors influencing the MTT-based colorimetric assays could be avoided. Cells were seeded at 8,000/well into 96-well plates, and allowed to adhere and spread for 20 hours in complete medium (with 10% FCS) in a CO_2 incubator. Consecutively, cells were washed, the medium was exchanged for DMEM with 2% FCS and 2 ng/ml PDGF-BB, various inhibitors were added as needed, and the plate was transferred to a 37°C, 5% CO_2 chamber on an Olympus IX81 inverted microscope. Time-lapse imaging was performed, taking one frame at every 10 minutes using an Olympus xcellence^RT system. Cells were counted at start and at 24 hours using the cell counter module of ImageJ [29]. Cell growth in 24 hours was expressed as multiple of initial cell numbers and plotted as mean ± SD (n=3). Inhibitors against the p38 MAPK, p42/44 MAPK, Erk5 and JNK kinase pathways were from Medchem Express Europe (Stockholm, Sweden) and used at their published biological IC_{50} concentrations as follows. SB203580 against p38 MAPK (15 µM), U0126 against MEK1/2 phosphorylating p42/44 MAPK (Erk1/2) (5 µM), BIX02188 against MEK 5 phosphorylating Erk5 (1 µM), SP600125 against JNK1,2,3 (10 µM), and Kobe0065 inhibiting activation of Raf by Ras (10 µM).

2.9. Measurement of cell motility

In order to measure cell motility, we used the Olympus xcellence^RT live cell imaging system with a 37°C, 5% CO_2 chamber on an Olympus IX81 inverted microscope. Cells were seeded in complete medium at 8,000 and 32,000 per well in 96-well plates and allowed to

adhere for 20 hours. The medium was exchanged for DMEM with 2% FCS and 2 ng/ml PDGF-BB, and cells were imaged at every 10 minutes for minimum 36 hours using a 10x objective with 645 nm/pixel resolution. The MTrackJ plugin [30] of ImageJ was used to track individual cells. The center of mass for each cell was tracked until the first mitotic event [31, 32]. Track data from three experiments ($n \geq 100$ for each condition) were exported and analyzed with the Chemotaxis and Migration Tool (v.2.0) from ibidi GmbH (Martinsried, Germany). The analyzed time span was increased from 100 min to 1500 min in 100 min steps to be able to account for the various times taken by each cell before mitosis (all observed cells divided before 1500 min). Accumulated distance and Euclidean distance (absolute displacement) were plotted as a function of observation time. Average velocity of cells did not change much with the length of observation time, and therefore the average velocities derived from the full length tracks were plotted. Graphs representing all cell tracks centered to start at coordinates (0,0) were plotted for 200, 500 and 1500 minutes observation time and overlaid for sparse and confluent cultures.

3. Results

3.1. Lipid raft localization of PDGFR-β in the cell membrane is a function of cell culture confluence

Preliminary experiments have shown that expression of PDGFR-β in A172 glioblastoma cells increases with confluence of cells in culture and that these receptors are mainly localized to GM1 rich lipid microdomains also termed lipid rafts. To quantitate the degree of overlap between clusters of PDGFR-β and submicron sized lipid rafts, we employed confocal microscopy yielding 1.5 micron thick optical slices of the upper cell membrane. Colocalization was quantified by calculating the cross correlation coefficient. Overlap of PDGFR with lipid rafts was directly proportional to the confluence of the monolayer, regardless of whether cells were seeded at varying densities and measured after having adhered to the substrate, or seeded at the same density, and left to grow continuously over several days to reach increasing levels of confluence (Figure 1A). This indicated that cell culture confluence as a state and not the process of reaching it regulates receptor expression and raft localization.

3.2. Phosphorylation of specific residues on PDGFR-β also depends on cell confluence and is a function of raft localization

To investigate whether the confluence dependent raft localization of the receptors has any functional consequence, we quantitated the amount of specific phosphotyrosine residues inside and outside GM1 rich membrane domains both in resting and PDGF-BB stimulated cells by immunofluorescence. We calculated the pixel by pixel distribution of specific phosphotyrosine residues both inside and outside lipid rafts. An example is shown in Figure 1B for the case of p-Tyr716 localized inside rafts. Here, sparse cultures exhibited basal phosphorylation of Tyr716 inside rafts slightly higher than confluent cultures, and showed a greatly increased activation upon stimulation with PDGF-BB, whereas the confluent cultures hardly increased p-Tyr716 in their rafts upon stimulus. Overall, we found that the mean of the log-normal distributions serves well to characterize the specific activation of the tyrosine residues of interest, namely that of Tyr716, Tyr751, Tyr771 and Tyr1021.

The means of histograms revealed a raft-dependent inverse pattern of activation of residues Tyr716 and Tyr771, which oppositely regulate the Ras-MAPK pathway, as a function of cell culture confluence. Following PDGF-BB stimulation, Tyr716 residues, responsible for activating the Ras-MAPK pathway, were mainly phosphorylated in sparse cultures, and a greater part of them in GM1 rich domains (Figure 1C). Tyr771 on the other hand, which negatively regulates the Ras-MAPK pathway through activating Ras-GAP, was more phosphorylated in confluent cultures, but also with a dominance of lipid raft-localized receptors (Figure 1D). Cell confluence had no prominent effect on the baseline activation of Tyr716 and Tyr771; overall, sparse cultures exhibited 1.3x and 0.9x the phosphorylation for these residues compared to confluent ones.

Basal phosphorylation of Tyr751 responsible for activating the PI3K-Akt pathway was 1.6x higher in sparse than in confluent cultures. Following PDGF-BB stimulus, sparse cells showed increased phosphorylation inside lipid rafts (Figure 1E). Tyr1021 phosphorylation, which triggers calcium response by activating PLCγ, was globally higher in GM1 rich membrane areas, and exhibited considerable increase upon ligand stimulation in confluent cells (Figure 1F).

The differences seen so far represent absolute p-Tyr levels in the vicinity of the membrane. However, to properly assess the role of lipid rafts in segregating phosphorylation-

dephosphorylation processes, we must also consider the trends in relative specific receptor phosphorylation. The image processing algorithm is depicted in Figure 2A. First, specific phosphotyrosine signal intensities were normalized pixel by pixel to the total PDGFR signal to obtain relative PDGFR phosphorylation in the cell membrane. Next, the binary mask created from thresholding the GM1 signal was used to generate the ratio of relative phosphorylation inside and outside GM1 rich domains. The added benefit of this approach is that differences in labeling intensities across independent experiments are equalized and thus several independent experiments can be cumulated (Figure 2A).

Figure 2B shows examples of triple labeling the PDGFR, one of its specific p-Tyr residues, and GM1 gangliosides. Processing these images using the double normalization approach (Figure 2A) highlights the role of lipid rafts in executing specific phosphorylation: upon PDGF stimulation, the specific phosphorylation of PDGFR normalized to total PDGFR was always higher inside rafts than outside rafts. This increase was restricted by the state of confluence and the tyrosine residue of interest. Residue Tyr716 (Figure 2C) activating the Ras-MAPK pathway was prominently phosphorylated in sparse cells, whereas Tyr771 (Figure 2D) inhibiting the same pathway was phosphorylated in confluent cells. Tyr751 (Figure 2E), stimulating the Akt kinase, showed increased relative phosphorylation in sparse cells. However, relative activation of Tyr1021, the docking site for PLCγ, was significantly higher in rafts of confluent cells (Figure 2F). These observations correlate well with data on absolute phosphorylation levels in Figure 1, and corroborate the idea that cell confluence influences the morphological segregation in lipid rafts and differential phosphorylation on specific tyrosine residues of PDGF receptors and thereby induces alternative cellular functions.

3.3. Activation of the Ras-MAPK pathway and consequential cell proliferation is dominant in sparse cultures

We performed Western blot analysis to confirm that the selective tyrosine phosphorylation depends on cell confluence and to test the activation of relevant downstream signaling pathways. To reveal whether the findings can be generalized, a second PDGFR expressing glioblastoma cell line, T98G, was also examined in addition to A172 cells.

In accordance with microscopy data, levels of p-Tyr716 which activates the Ras-MAPK pathway showed a transient increase in sparse cultures of both cell lines following PDGF-BB ligand stimulation, and no change in confluent cells. Conversely, increased phosphorylation of the Tyr771 residue activating Ras-GAP, an inhibitor of the pathway, was more prominent

in confluent cultures, although some transient phosphorylation was also seen in sparse cultures. Next, we measured the phosphorylation of two effector MAPK isoforms, p38 MAPK, and p42/p44 MAPK. Coherent with the specific phosphorylation of tyrosine residues activating and inhibiting these MAP kinases, both p38 and p42/p44 were activated mainly in sparse cultures. We have observed a time delay between the activation of receptors and effector proteins: while Tyr 716 and Tyr 771 residues were maximally phosphorylated within 1-2 minutes of ligand stimulus, and by 15 min were already back to baseline; activation of effector MAP kinases peaked in the range of 5 – 30 minutes, land lasted through the 60 min observation period (Figure 3A).

Since activation of the MAP kinase pathway is expected to influence cell proliferation; accumulation of the Ki-67 proliferation marker in cell nuclei was also assessed by fluorescence microscopy. In line with increased MAPK activation in sparse cultures, we found greatly increased Ki-67 protein levels in the nuclear region of ~ 85% of the cells in sparse cultures two hour after PDGF stimulus. Coherent with low MAPK activation, the proportion of highly Ki-67 positive cells was only 1% in confluent cultures, and a further 12% exhibited a slight increase. Without stimulus, no signs of proliferation were detected in either state of the serum starved cell cultures (Figure 3B).

We have used an MTT based assay to show direct evidence of increased proliferation in sparse cultures. Both A172 and T98G cells were seeded at densities in the range of 9,000/cm^2 to 150,000/cm^2 and final cell number normalized to initial cell number was plotted as a function of seeding density. As evident from Figure 4A, the lowest density cultures of both A172 and T98G nearly doubled in two days, proliferation gradually dropped with increasing initial cell numbers, and cell cultures with very high seeding density did not grow in terms of metabolic activity, or even showed decreased MTT oxidation.

We also showed how the time course of proliferation rates differ for the confluent and sparse cultures of T98G cells using impedance based real time cell adhesion (RTCA) measurements. Figure 4B shows the increasing surface coverage of these cells as a function of time. During the first 20 hours, as confirmed by live cell microscopy, the cells first attach, and then start spreading on the substrate (marked by the black arrow). Once spreading is finished (dashed arrow), they start proliferation. The rate of proliferation (the slope of surface coverage normalized to initial cell number vs. time) is much greater for sparse cultures. One should note that without normalization to initial cell number (a factor of 4 between spares and

confluent cells), the impedance is of course higher for confluent cultures, but the relation of slopes remains the same. In addition confluent cultures saturate the well sooner and no further increase of impedance can be detected.

3.4. Multiple MAP kinases are responsible for the proliferation

To show the contribution of the various MAPKs to cell proliferation, we applied specific inhibitors of the p38 MAPK, p42/44 MAPK, Erk5 and JNK pathways (Figure 4C). We found that in A172 cells inhibition of p38 MAPK with the published biological EC50 dose of SB203580 decreased the proliferation by ~75%, while inhibiting the p42/44 MAPK pathway through MEK1/2 by U0126 caused only ~30% decrease. Combination of the two inhibitors, however, caused nearly complete inhibition. T98G cells behaved differently, and inhibition of p38 and p42/44 MAPK pathways resulted in only ~10% and ~35% decrease of proliferation, and their combination appeared additive. Consequently, we have also tested BIX02188 to inhibit Erk5 via MEK5, SP600125 to inhibit the JNK kinases, and Kobe0065 to inhibit the Ras/Raf interaction which can serve as a starting point of these cascades, when activated by the phosphorylation of Tyr716. At known biological EC50 doses, inhibition of Erk5 and JNK was ~60% and ~ 35% effective against proliferation of A172 and T98G. When all four MAPK families were inhibited, a complete block of proliferation occurred in both cell lines, similarly to the case where the initial activation step of Raf by Ras was inhibited.

3.5. Activation of the Akt survival kinase shows similar patterns in sparse and confluent cultures

Western blotting also confirmed that ligand stimulation induced phosphorylation of Tyr751 residues under both sparse and confluent growth conditions (Figure 5A). Tyr751 phosphorylation feeding into the PI3K pathway started within a minute of stimulation, decayed almost to background after an hour, and was somewhat higher in sparse cultures than in confluent ones. However, Akt phosphorylation did not show marked corresponding differences, possibly because of the multiplicity of various inputs targeting the Akt pathway. Consequently, we observed no significant tendentious differences in the spontaneous apoptotic rate and in heat-shock induced apoptosis of sparse versus confluent cells (data not shown).

3.6. Activation of the PLCγ pathway and consequential cell migration is dominant in confluent cultures

Phosphorylation of Tyr1021 occurred both in sparse and confluent cells, started by the first minute of stimulation, but was over within half an hour. Confluent cells showed markedly higher p-Tyr1021 than sparse cells of both cell lines. The phosphorylation of RhoA, an important effector activated along the PLCγ / PKC pathway, was correspondingly also greatly increased in confluent cells, while in sparse cells it remained at baseline with only a slight increase at 2-15 minutes. Immunofluorescence images in Figure 5B (top row) also show that two hours after stimulation RhoA phosphorylation can even be below the baseline seen in unstimulated cells, while in confluent cells it is still maintained at a very high level.

Based on this observation, we hypothesized that activation of the PLCγ pathway in confluent cells has a functional consequence on cell migration. Cortactin is an important protein facilitating polymerization and rearrangement of the actin cytoskeleton, promoting the formation of lamellipodia, invadopodia, and cell migration. Figure 5B shows that cellular localization and rearrangement of this protein to the leading edges were oppositely regulated in sparse and confluent cultures. In resting sparse cells, cortactin was mostly localized to the polarized cell front protrusion but decreased in quantity and appeared perinuclearly two hours after stimulus. In unstimulated confluent cultures, cortactin dominantly showed cytoplasmic localization, but following PDGF-BB stimulation, it cumulated in the polarized leading cell front.

For a functional assay, next we directly monitored and quantitatively analyzed cell motility using live cell microscopy and tracking. This assay complies well with our model where no chemotactic gradient is implied, yet migration rate of cells increases with their local density. Figure 6A shows the tracks of observed cells centered to start at coordinates (0,0), with tracks of sparse cells (in red) overlaid the tracks of confluent cells (in black). Owed to tracks ending with the mitotic event at various time points, cumulated tracks are plotted for 200, 500 and 1500 minutes observation time to give a broader picture of migratory tendencies for both A172 and T98G cells. It is very clear that confluent cultures of both cell lines show increased migration at all time points. Accumulated distance (Figure 6B) and Euclidean distance (absolute displacement, Figure 6C) were plotted as a function of cumulative observation time in 100 minute steps. As expected from the cell tracks, confluent cultures of both cell lines covered at least twice longer distances over the same time, got at least twice further from their

starting point. Since with time more and more cell tracks ended due to mitosis, both these plots flatten to a plateau. The sparse cultures reach the plateau sooner; the linear phase for confluent cells is longer, coherent with divisions occurring sooner on average in sparse cultures. Average velocity was also higher in confluent cultures, and did not change over time; therefore only the overall averages were plotted (Figure 6D).

4. Discussion

Earlier we have observed that PDGF stimulated glioblastoma cells respond with a two-phase calcium signal constituted of intracellular release followed by sustained influx from the extracellular space [28, 33]. Interestingly, as opposed to confluent cells, those in sparse cultures mostly displayed a reduced response; shorter, lower spikes, or no transients at all [27]. It has also been known for long [24] that normal cells undergo contact inhibition, while malignant transformation often abrogates this regulatory feature of mammalian cells. While there are various proposed mechanisms of contact inhibition [34-36], the idea of a confluence dependent regulatory mechanism immediately at the first branching level of the input signal through receptor tyrosine kinases seemed compelling. In fact, we have observed that a differential phosphorylation of several tyrosine residues of PDGFR-β receptors was evoked by PDGF stimulation in glioblastoma cells as a function of cell confluence.

This differential phosphorylation took place primarily in GM1-rich lipid rafts, regardless of the residue concerned, which is coherent with the ample evidence cumulated in the literature that lipid rafts serve as organizing platforms for growth factor receptors [19, 21, 23, 37]. While there was a gradual increase of receptor expression with cell confluence (data not shown), and a parallel increase of the raft-localization of these receptors, even in the sparse state, more phosphorylated tyrosine residues were found in lipid rafts, as evidenced by our microscopic pixel-by-pixel quantitation algorithm. The major difference was the identity of the residue. Some of the examined residues were predominantly activated in sparse cells, yet others in confluent ones.

In sparse cultures, both absolute and relative phosphorylation of tyrosine 716 specific to the Ras/MAPK pathway and tyrosine 751 specific to the PI3-kinase/Akt pathway [10] were increased upon ligand stimulation, dominantly in GM1 rich clusters of the cell membrane. On the other hand, in confluent cultures, tyrosine 771 that serve as an adaptor for Ras-GAP inactivating the MAPK pathway [12], and tyrosine 1021 feeding into the PLCγ/PKC pathway [16] were the ones that showed significant phosphorylation. These findings in single cell microscopy were confirmed for cell populations by Western blotting.

Western blotting was then also used to verify that consecutive downstream steps in signaling are coherent with the differential phosphorylation of tyrosine residues. As logically expected, phosphorylated p38-MAPK, and also p42/44-MAPK were increased in sparse cultures upon PDGF stimulus, in coherence with increased Tyr716 phosphorylation. Meanwhile, in confluent cells, MAPK phosphorylation was low, partly owed to the lower levels of p-Tyr716, and partly to the strong phosphorylation of Tyr771, which inhibits the MAPK pathway by activating Ras-GAP. In confluent cells, increased phosphorylation of Tyr1021 not only yielded a two-phase calcium signal as observed formerly [27], but also enhanced RhoA phosphorylation likely as a result of PKC activation [38]. Regarding Akt phosphorylation, we have not seen major differences between confluent and sparse cells, which is probably the result of the very many diverse inputs that lead to Akt phosphorylation and pro-survival signaling, and is also a reasonable finding considering that both migrating and proliferating tumor cells need antiapoptotic signals.

As a proof of concept, at the molecular level we have looked at functional-morphological markers of proliferation and migration: Ki-67 with nuclear localization and cortactin in the leading edge. The majority of sparse cells stimulated with PDGF exhibited a high level of nuclear Ki-67 immunoreactivity, coherent with the activated proliferation pathways. At the same time, in confluent cells, nuclear Ki-67 signal was hardly visible. However, these cells showed marked pRhoA immunoreactivity also in fluorescence microscopy, paralleled with an accented cortactin signal in leading edges. On the contrary, sparse cells have lost even those cortactin-rich protrusions upon stimulus that were visible at rest.

To verify the altered cellular functions, the proliferation rates and motilities of sparse and confluent cultures have been compared. As revealed by metabolic and real time cell adhesion assays, sparse cells proliferated at greater rate than confluent ones; for these latter, live cell imaging confirmed that the first mitotic events occurred later. Specific inhibitors of members of the MAP kinase family revealed that to some extent Erk5 and JNK are also involved in the proliferative response and that while A172 cells heavily rely on p38 MAPK in this aspect, T98G cells need to have all MAPK families inhibited for a complete proliferation block. As expected, inhibition of the MAPK pathway at its input of Ras/Raf interaction totally abolished proliferation in both cell lines. Live cell imaging also revealed that migration velocity and total accumulated distance were greater in confluent cultures by a factor of 2 and 4 for A172 and T98G, and total displacement was greater by a factor >2 for both. Overall, the final cellular responses observed were coherent with the initial differential phosphorylation of the PDGF receptor β.

Such differential phosphorylation is not likely to be implemented directly during receptor activation and transphosphorylation, rather, one possible explanation is the active, and confluence dependent participation of phosphatases. Regulation of PDGFR by phosphotyrosine-phosphatases is known in quite some detail [39-41]. Based on these investigations, PTPN1, PTPN4, and PTPN11 [42, 43] are the best candidates for differentially dephosphorylating the tyrosine residues of activated receptors. It remains to be seen whether these are regulated by cell confluence at the level of expression, activity, or raft/non-raft redistribution.

5. Conclusions

Cumulatively, our observations suggest that the same stimulus is able to promote distinct signaling outputs through a regulatory mechanism driven by cell confluence and based on segregation in lipid rafts. These altered outputs are highly relevant for tumor proliferation and spreading. Specifically, cell division dominates in sparse cultures and promotion of migration is accompanied by a mitigated proliferative response in confluent monolayers showing contact inhibition. This mechanism could be a genuine strategy of tumor cells to use the same signaling machinery for providing responses optimized for their environmental circumstances, and is not restricted to a single cell line, as both A172 and T98G behaved in a similar manner, with minor differences only in the time-course of activation processes and the spectrum of relevant MAPK kinases. On the other hand, non-malignant primary fibroblasts, such as the AG01523B, expressing the same PDGFR-β in their membrane, do not show responses optimized for continuous proliferation and spreading, contact inhibited cells do not start to migrate (data not shown).

From the pathological perspective, our experiments reveal the differential phosphorylation of important tyrosine residues on the PDGF receptor tyrosine kinase in the membrane of confluent and sparse cells, in spite of both types of cells encountering the very same PDGF-BB stimulus. The differentially phosphorylated residues activate their respective relevant downstream pathways, which evoke, depending on the state of cell confluence, a cellular response which is very logical from the point of view of an invasive tumor. Densely packed cells modeling the lack of space in locally growing tumors respond to stimulus by migration, an important step on the route to invasion or metastasis, while sparse cells, modeling freshly settled disseminated tumor cells respond to the same stimulus by vigorous proliferation.

Declaration of conflict of interests: None of the authors have conflicts interest.

Acknowledgements

We acknowledge the financial support from the Hungarian Scientific Research Fund (OTKA K75752, NK 101337), and the Baross Gabor Program (REG-EA-09-1-2009-0010). We wish to thank Eszter Molnár and Tamás Garay at the 2nd Dept. of Pathology, Semmelweis University, Budapest, Hungary, for running a pilot experiment on cell migration. We also are grateful to József Tóvári (Department of Experimental Pharmacology, National Institute of Oncology, Budapest, Hungary) for valuable discussion on cell migration.

References

1. Heldin CH, Westermark B: **Mechanism of action and in vivo role of platelet-derived growth factor.** *Physiol Rev* 1999, **79:**1283-1316.
2. Ren H, Yang BF, Rainov NG: **Receptor tyrosine kinases as therapeutic targets in malignant glioma.** *Rev Recent Clin Trials* 2007, **2:**87-101.
3. Nister M, Claesson-Welsh L, Eriksson A, Heldin CH, Westermark B: **Differential expression of platelet-derived growth factor receptors in human malignant glioma cell lines.** *J Biol Chem* 1991, **266:**16755-16763.
4. Smith D, Shimamura T, Barbera S, Bejcek BE: **NF-kappaB controls growth of glioblastomas/astrocytomas.** *Mol Cell Biochem* 2008, **307:**141-147.
5. Mapstone TB: **Expression of platelet-derived growth factor and transforming growth factor and their correlation with cellular morphology in glial tumors.** *J Neurosurg* 1991, **75:**447-451.
6. Shih AH, Dai C, Hu X, Rosenblum MK, Koutcher JA, Holland EC: **Dose-dependent effects of platelet-derived growth factor-B on glial tumorigenesis.** *Cancer Res* 2004, **64:**4783-4789.
7. Majumdar K, Radotra BD, Vasishta RK, Pathak A: **Platelet-derived growth factor expression correlates with tumor grade and proliferative activity in human oligodendrogliomas.** *Surg Neurol* 2009, **72:**54-60.
8. Camorani S, Esposito CL, Rienzo A, Catuogno S, Iaboni M, Condorelli G, de Franciscis V, Cerchia L: **Inhibition of receptor signaling and of glioblastoma-derived tumor growth by a novel PDGFRbeta aptamer.** *Molecular therapy : the journal of the American Society of Gene Therapy* 2014, **22:**828-841.
9. Arvidsson AK, Rupp E, Nanberg E, Downward J, Ronnstrand L, Wennstrom S, Schlessinger J, Heldin CH, Claesson-Welsh L: **Tyr-716 in the platelet-derived growth factor beta-receptor kinase insert is involved in GRB2 binding and Ras activation.** *Mol Cell Biol* 1994, **14:**6715-6726.
10. Venkatesan B, Ghosh-Choudhury N, Das F, Mahimainathan L, Kamat A, Kasinath BS, Abboud HE, Choudhury GG: **Resveratrol inhibits PDGF receptor mitogenic signaling in mesangial cells: role of PTP1B.** *Faseb J* 2008, **22:**3469-3482.
11. Kashishian A, Kazlauskas A, Cooper JA: **Phosphorylation sites in the PDGF receptor with different specificities for binding GAP and PI3 kinase in vivo.** *Embo J* 1992, **11:**1373-1382.
12. Ekman S, Kallin A, Engstrom U, Heldin CH, Ronnstrand L: **SHP-2 is involved in heterodimer specific loss of phosphorylation of Tyr771 in the PDGF beta-receptor.** *Oncogene* 2002, **21:**1870-1875.

13. Courtneidge SA, Kypta RM, Cooper JA, Kazlauskas A: **Platelet-derived growth factor receptor sequences important for binding of src family tyrosine kinases.** *Cell Growth Differ* 1991, **2:**483-486.
14. Valius M, Kazlauskas A: **Phospholipase C-gamma 1 and phosphatidylinositol 3 kinase are the downstream mediators of the PDGF receptor's mitogenic signal.** *Cell* 1993, **73:**321-334.
15. Datta SR, Brunet A, Greenberg ME: **Cellular survival: a play in three Akts.** *Genes Dev* 1999, **13:**2905-2927.
16. Kundra V, Escobedo JA, Kazlauskas A, Kim HK, Rhee SG, Williams LT, Zetter BR: **Regulation of chemotaxis by the platelet-derived growth factor receptor-beta.** *Nature* 1994, **367:**474-476.
17. Rhee SG: **Regulation of phosphoinositide-specific phospholipase C.** *Annu Rev Biochem* 2001, **70:**281-312.
18. Reddi AL, Ying G, Duan L, Chen G, Dimri M, Douillard P, Druker BJ, Naramura M, Band V, Band H: **Binding of Cbl to a phospholipase Cgamma1-docking site on platelet-derived growth factor receptor beta provides a dual mechanism of negative regulation.** *J Biol Chem* 2007, **282:**29336-29347.
19. Nagy P, Vereb G, Sebestyen Z, Horvath G, Lockett SJ, Damjanovich S, Park JW, Jovin TM, Szollosi J: **Lipid rafts and the local density of ErbB proteins influence the biological role of homo- and heteroassociations of ErbB2.** *J Cell Sci* 2002, **115:**4251-4262.
20. Pike LJ: **Growth factor receptors, lipid rafts and caveolae: an evolving story.** *Biochim Biophys Acta* 2005, **1746:**260-273.
21. Vereb G, Szollosi J, Matko J, Nagy P, Farkas T, Vigh L, Matyus L, Waldmann TA, Damjanovich S: **Dynamic, yet structured: The cell membrane three decades after the Singer-Nicolson model.** *Proc Natl Acad Sci U S A* 2003, **100:**8053-8058.
22. Harder T, Simons K: **Clusters of glycolipid and glycosylphosphatidylinositol-anchored proteins in lymphoid cells: accumulation of actin regulated by local tyrosine phosphorylation.** *Eur J Immunol* 1999, **29:**556-562.
23. Vereb G, Matko J, Vamosi G, Ibrahim SM, Magyar E, Varga S, Szollosi J, Jenei A, Gaspar R, Jr., Waldmann TA, Damjanovich S: **Cholesterol-dependent clustering of IL-2Ralpha and its colocalization with HLA and CD48 on T lymphoma cells suggest their functional association with lipid rafts.** *Proc Natl Acad Sci U S A* 2000, **97:**6013-6018.
24. Fisher HW, Yeh J: **Contact inhibition in colony formation.** *Science* 1967, **155:**581-582.
25. Thiery JP: **Epithelial-mesenchymal transitions in tumour progression.** *Nat Rev Cancer* 2002, **2:**442-454.
26. Fiaschi T, Chiarugi P, Buricchi F, Giannoni E, Taddei ML, Talini D, Cozzi G, Zecchi-Orlandini S, Raugei G, Ramponi G: **Low molecular weight protein-tyrosine phosphatase is involved in growth inhibition during cell differentiation.** *J Biol Chem* 2001, **276:**49156-49163.
27. Vereb G, Feuerstein BG, Hyun WC, Fulwyler MJ, Balazs M, Szollosi J: **Biphasic calcium response of platelet-derived growth factor stimulated glioblastoma cells is a function of cell confluence.** *Cytometry A* 2005, **67:**172-179.
28. Szollosi J, Feuerstein BG, Vereb G, Pershadsingh HA, Marton LJ: **Calcium channels in PDGF-stimulated A172 cells open after intracellular calcium release and are not voltage-dependent.** *Cell Calcium* 1991, **12:**477-491.
29. Rasband WS: **ImageJ.** *U S National Institutes of Health, Bethesda, Maryland, USA* 1997-2014.
30. Meijering E, Dzyubachyk O, Smal I: **Methods for cell and particle tracking.** *Methods in enzymology* 2012, **504:**183-200.

31. Garay T, Juhasz E, Molnar E, Eisenbauer M, Czirok A, Dekan B, Laszlo V, Hoda MA, Dome B, Timar J, et al: **Cell migration or cytokinesis and proliferation?--revisiting the "go or grow" hypothesis in cancer cells in vitro.** *Experimental cell research* 2013, **319:**3094-3103.
32. Tovari J, Futosi K, Bartal A, Tatrai E, Gacs A, Kenessey I, Paku S: **Boyden chamber-based method for characterizing the distribution of adhesions and cytoskeletal structure in HT1080 fibrosarcoma cells.** *Cell adhesion & migration* 2014, **8:**509-516.
33. Vereb G, Jr., Szollosi J, Matyus L, Balazs M, Hyun WC, Feuerstein BG: **Depletion of intracellular calcium stores facilitates the influx of extracellular calcium in platelet derived growth factor stimulated A172 glioblastoma cells.** *Cytometry* 1996, **24:**64-73.
34. Takai Y, Miyoshi J, Ikeda W, Ogita H: **Nectins and nectin-like molecules: roles in contact inhibition of cell movement and proliferation.** *Nat Rev Mol Cell Biol* 2008, **9:**603-615.
35. Wieser RJ, Schutz S, Tschank G, Thomas H, Dienes HP, Oesch F: **Isolation and characterization of a 60-70-kD plasma membrane glycoprotein involved in the contact-dependent inhibition of growth.** *J Cell Biol* 1990, **111:**2681-2692.
36. Moh MC, Shen S: **The roles of cell adhesion molecules in tumor suppression and cell migration: a new paradox.** *Cell adhesion & migration* 2009, **3:**334-336.
37. de Laurentiis A, Donovan L, Arcaro A: **Lipid rafts and caveolae in signaling by growth factor receptors.** *Open Biochem J* 2007, **1:**12-32.
38. Su T, Straight S, Bao L, Xie X, Lehner CL, Cavey GS, Teknos TN, Pan Q: **PKC epsilon Phosphorylates and Mediates the Cell Membrane Localization of RhoA.** *ISRN oncology* 2013, **2013:**329063.
39. Kovalenko M, Denner K, Sandstrom J, Persson C, Gross S, Jandt E, Vilella R, Bohmer F, Ostman A: **Site-selective dephosphorylation of the platelet-derived growth factor beta-receptor by the receptor-like protein-tyrosine phosphatase DEP-1.** *J Biol Chem* 2000, **275:**16219-16226.
40. Markova B, Herrlich P, Ronnstrand L, Bohmer FD: **Identification of protein tyrosine phosphatases associating with the PDGF receptor.** *Biochemistry* 2003, **42:**2691-2699.
41. Persson C, Savenhed C, Bourdeau A, Tremblay ML, Markova B, Bohmer FD, Haj FG, Neel BG, Elson A, Heldin CH, et al: **Site-selective regulation of platelet-derived growth factor beta receptor tyrosine phosphorylation by T-cell protein tyrosine phosphatase.** *Mol Cell Biol* 2004, **24:**2190-2201.
42. Dagnell M, Frijhoff J, Pader I, Augsten M, Boivin B, Xu J, Mandal PK, Tonks NK, Hellberg C, Conrad M, et al: **Selective activation of oxidized PTP1B by the thioredoxin system modulates PDGF-beta receptor tyrosine kinase signaling.** *Proc Natl Acad Sci U S A* 2013, **110:**13398-13403.
43. Wu JH, Goswami R, Cai X, Exum ST, Huang X, Zhang L, Brian L, Premont RT, Peppel K, Freedman NJ: **Regulation of the platelet-derived growth factor receptor-beta by G protein-coupled receptor kinase-5 in vascular smooth muscle cells involves the phosphatase Shp2.** *J Biol Chem* 2006, **281:**37758-37772.

Figure Legends

Figure 1

Residue-specific phosphorylation of PDGFR-β is confluence and lipid raft dependent

A: Raft localization of PDGFR receptors as a function of cell confluence. Schematic drawing on the left indicates the position of confocal slice in the cell used for analysis. Images (from a 14.6x14.6 μm^2 area) show localization and visual colocalization of PDGF receptors (red) and GM1-rich lipid rafts (green) in A172 cells. Cross-correlation coefficients in the graph below indicate the extent of colocalization as a function of cell density. Data are averages of the cross-correlation coefficient ± SEM of 40–60 cells from 3 independent experiments.

B: Quantitation of specific tyrosine phosphorylation in microscopic images. For an example, pixel-by-pixel intensity distribution of p-Tyr716 inside lipid rafts is shown here as a function of cell confluence and PDGF-BB stimulus. The confocal images (21.3x21.3 μm^2) show lipid rafts in green, and p-Tyr716 in blue.

C; D; E and F: Specific tyrosine phosphorylation as function of cell confluence and PDGF-BB stimulus. Mean pixel intensities before and after 20 ng/ml PDGF-BB stimulation are derived from of the intensity distribution curves exemplified in **B**. Sparse (open columns) and confluent (filled columns) cultures were of densities 2 x 10^4 cells/cm^2 and 1 x 10^5 cells/cm^2. p-Tyr716 (C), p-Tyr771 (D), p-Tyr751 (E) and p-Tyr1021 (F) were quantitated both inside and outside lipid rafts.

Figure 2

Quantitative analysis of relative specific receptor phosphorylation in membrane microdomains

A: Digital image processing algorithm for quantitative characterization of relative specific receptor phosphorylation in the cell membrane. An example is shown for labeling total (red) and tyrosine phosphorylated (blue) receptors as well as lipid rafts (green), and using the lipid raft image as a binary mask for deriving an numeric characterizing raft vs. non-raft based relative specific phosphorylation status independent of labeling and detection efficiency.

B: Confocal images provide information about the membrane distribution of cell surface receptors (red), specific phosphotyrosine residues (blue) and lipid rafts (green). The

images (21.3x21.3 μm^2) taken after 2 min stimulation with 20 ng/ml PDGF-BB show that in A172 glioblastoma PDGFR, p-Tyr716 and p-Tyr751 colocalize with GM1 rich domains of the sparse cultures, while p-Tyr771 and p-Tyr1021 are more abundant in rafts of confluent cultures, as indicated by stronger intensities and more white spots where the three label colors colocalize.

C; D; E and F: Ratio of raft and non-raft specific relative receptor tyrosine phosphorylation. Sparse (open columns) and confluent (filled columns) cultures were of densities 2 x 10^4 cells/cm^2 and 1 x 10^5 cells/cm^2, respectively. p-Tyr716 (C), p-Tyr771 (D), p-Tyr751 (E) and p-Tyr1021 (F) were quantitated before and 2 min after stimulation with 20 ng/ml PDGF-BB. Data are averages of the ratios ± SEM of 40–60 cells from 3 independent experiments.

Figure 3

Proliferative signal routes are boosted in sparse and suppressed in confluent cultures

A: Western blot analysis of various phosphorylated proteins involved in MAPK signaling as a function of post-stimulus time. Following 0, 1 , 2, 5, 15, 30 and 60 minutes stimulation with 20 ng/ml PDGF-BB, phosphorylated Tyr716, Tyr771, p38 and p42/p44 MAPK were probed in sparse (1 x 10^4 cells/cm^2) and confluent (1 x 10^5 cells/cm^2) A172 and T98G glioblastoma cell cultures. Anti-β-actin antibody was used as loading control in addition to equalizing total protein in the samples.

B: Quantitation of proliferation induced by PDGF-BB treatment. Immunofluorescent analysis of Ki-67 (blue) shows proliferating cells in sparse (2 x 10^4 cells/cm^2) and confluent (1 x 10^5 cells/cm^2) A172 glioblastoma cultures. Propidium iodide was used to visualize all nuclei of the microscopic field (red). The images (117x117 μm^2) taken after a 2-hour stimulation with 20 ng/ml PDGF-BB show that Ki-67 activation increased in the nuclear region of ~ 85% of the cells in sparse cultures.

Figure 4

Cellular outcome of increased proliferative signaling in sparse cultures and its dependence on various MAP kinase pathways

A: Cell proliferation as a function of cell density

Cells plated at various densities (9,000 through 150,000/cm^2) were grown in 96-well plates for 2 days. Readout of the MTT-based assay was calibrated to know numbers of freshly

adhered viable cells of the same type, averaged for 6 measurements, normalized to the initially seeded cell number and plotted as its function.

B: Real time cell proliferation as a function of cell density

Real time cell adherence assay (RTCA) was done on T98G cells seeded to be sparse (15,000/cm^2) or confluent (60,000/cm^2) using an ECIS ZΘ analyzer. The measured impedance at any time point is proportional to the area of the electrode covered by cells. Impedance values from 4 wells were averaged, normalized to initial cell number, and plotted as a function of time. Black arrow: end of attachment phase, dashed arrow: end of spreading on substrate and beginning of proliferation.

C: Effect of inhibiting MAPK pathways on cell proliferation

Cells were seeded at 8,000/well into 96-well plates, allowed to adhere and spread for 20 hours then stimulated with 2 ng/ml PDGF-BB in the absence or presence of various specific inhibitors: SB203580 against p38 MAPK (15 μM), U0126 against MEK1/2 phosphorylating p42/44 MAPK (5 μM), BIX02188 against MEK 5 phosphorylating Erk5 (1 μM), SP600125 against JNK1,2,3 (10 μM), and Kobe0065 inhibiting activation of Raf by Ras (10 μM). Cells were imaged using an Olympus xcellence^RT system for 24 hours and cell growth was expressed as multiple of initial cell numbers and plotted as mean ± SD (n=3).

Figure 5

Confluent, but not sparse, cell cultures exhibit molecular signs of stimulus induced migratory response

A: Western blot analysis of various phosphorylated proteins involved in PI3-K and PLCγ signaling as a function of post-stimulus time. Following 0, 1 , 2, 5, 15, 30 and 60 minutes stimulation with 20 ng/ml PDGF-BB, phosphorylated Tyr751, Tyr1021, Akt and RhoA were probed in sparse (1 x 10^4 cells/cm^2) and confluent (1 x 10^5 cells/cm^2) A172 and T98G glioblastoma cell cultures. Anti-β-actin antibody was used as loading control in addition to equalizing total protein in the samples.

B: **Visualization of proteins involved in cell migration after PDGF-BB treatment.** Immunofluorescent labeling of phospho-RhoA (blue) and cortactin (red) in sparse (2 x 10^4 cells/cm^2) and confluent (1 x 10^5 cells/cm^2) A172 glioblastoma cell cultures before, and 2 hours after 20 ng/ml PDGF-BB stimulus shows increased migratory signaling in confluent, and decreased signaling in sparse cultures after PDGFR activation. Images are from 87.6x87.6 μm^2 fields of view.

Figure 6

Live cell imaging as functional proof of increased motility in confluent cultures

Cells seeded at 8,000 and 32,000 per well were stimulated with 2 ng/ml PDGF-BB and imaged after adhesion and spreading for minimum 36 hours taking one frame at every 10 minutes and tracked until their first division.

A: Tracks of A172 and T98G cells at various cumulative time points

Graphs representing all (≥100) cell tracks centered to start at coordinates (0,0) were plotted for 200, 500 and 1500 minutes observation time. Tracks of sparse cells (in red) were overlaid the tracks of confluent cells (in black).

B: Accumulated migration distance as a function of accumulation time

Accumulated distance was plotted as a function of accumulation time, increased in 100 minute steps. A172 cells are represented with black plots, T98G with red, confluent cells are shown with squares, sparse ones with circles. Data are mean of ≥100 cells ± SEM from three experiments.

C: Euclidean distance as a function of accumulation time

Euclidean distance (absolute displacement from the starting point) was plotted as a function of accumulation time, increased in 100 minute steps. A172 cells are represented with black plots, T98G with red, confluent cells are shown with squares, sparse ones with circles. Data are mean of ≥100 cells ± SEM from three experiments.

D: Migration velocity in sparse and confluent cultures

Migration velocity is plotted as a function cell type and confluence. Data are mean of ≥100 cells ± SEM from three experiments.

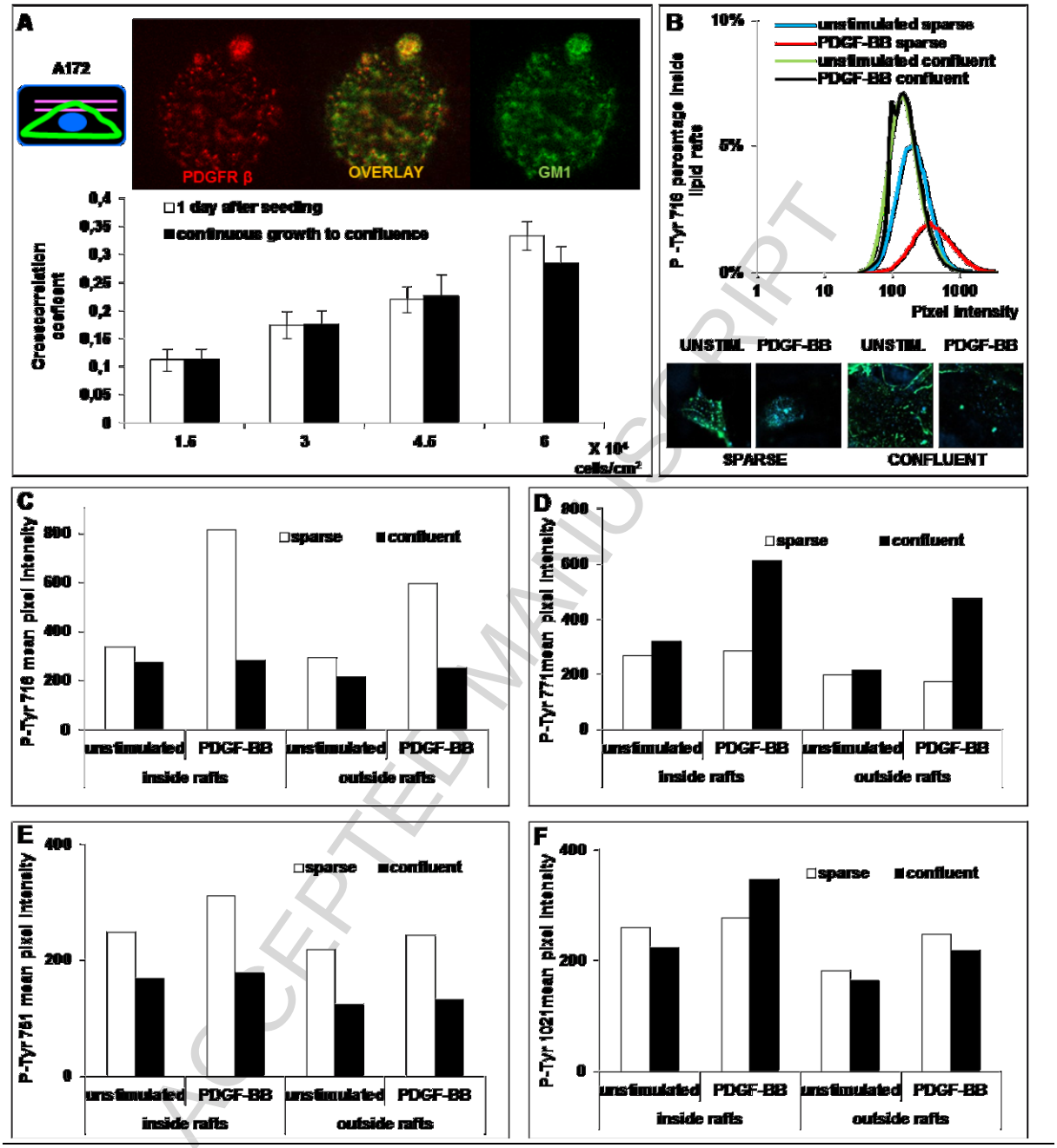

Figure 1

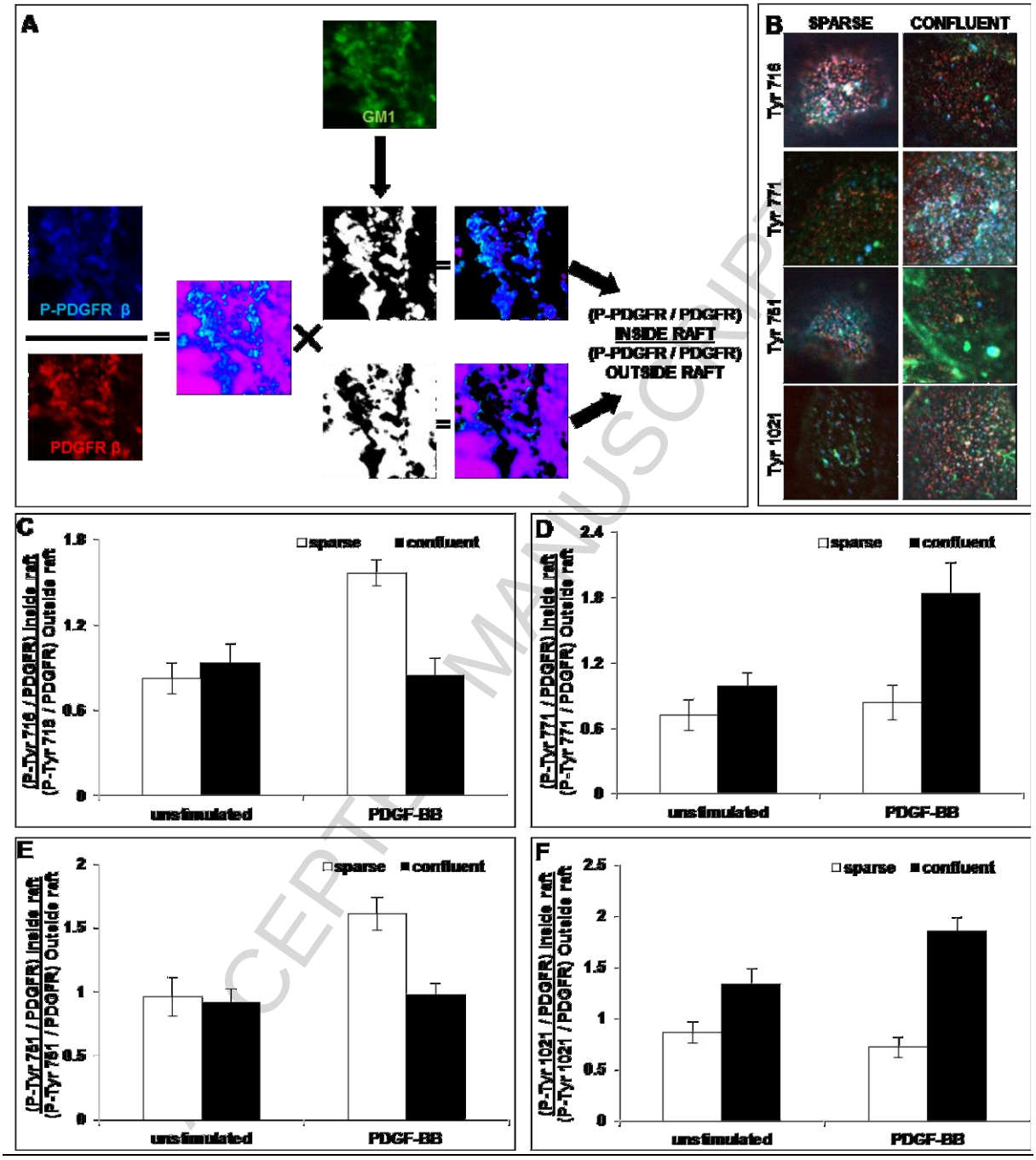

Figure 2

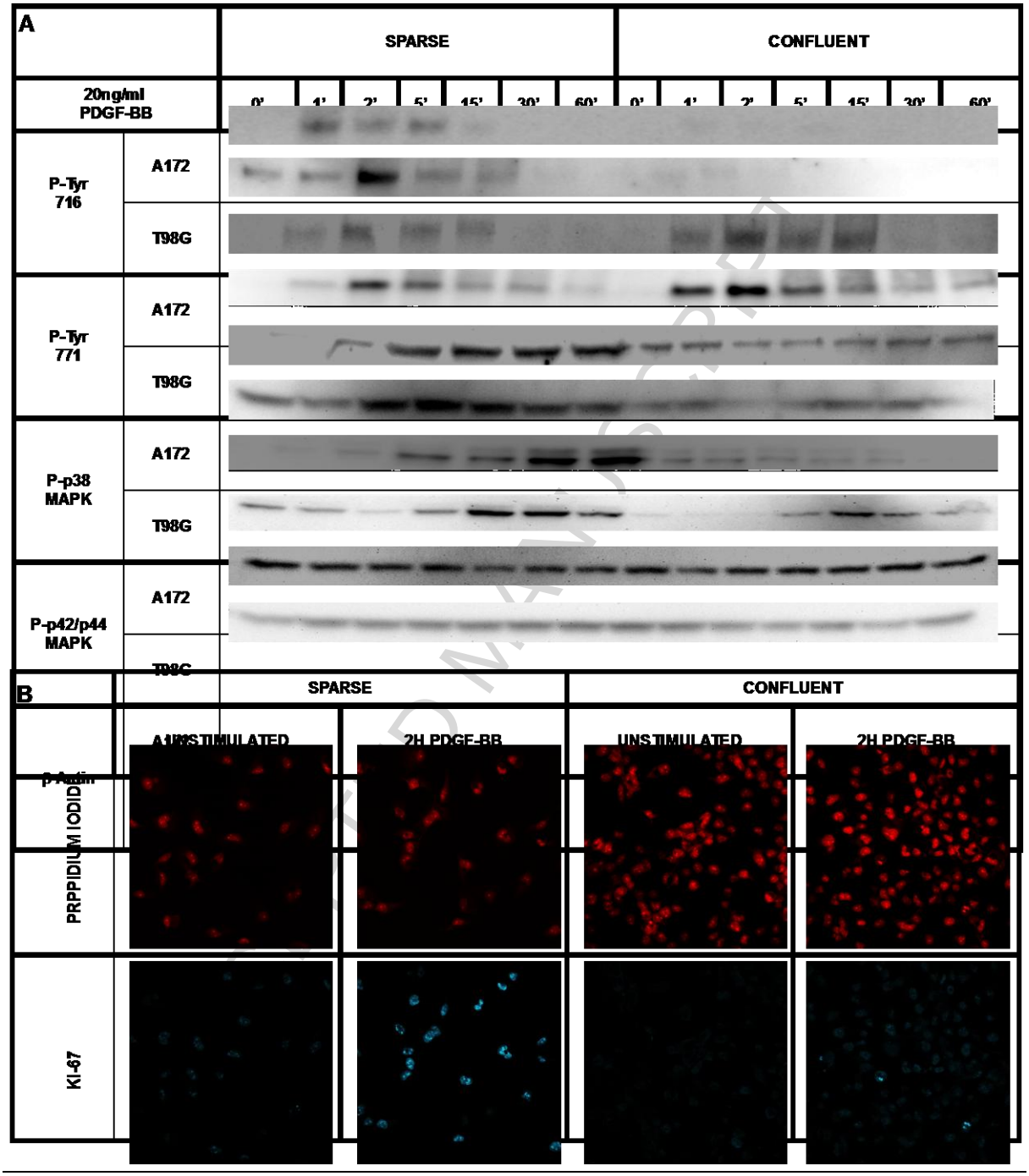

Figure 3

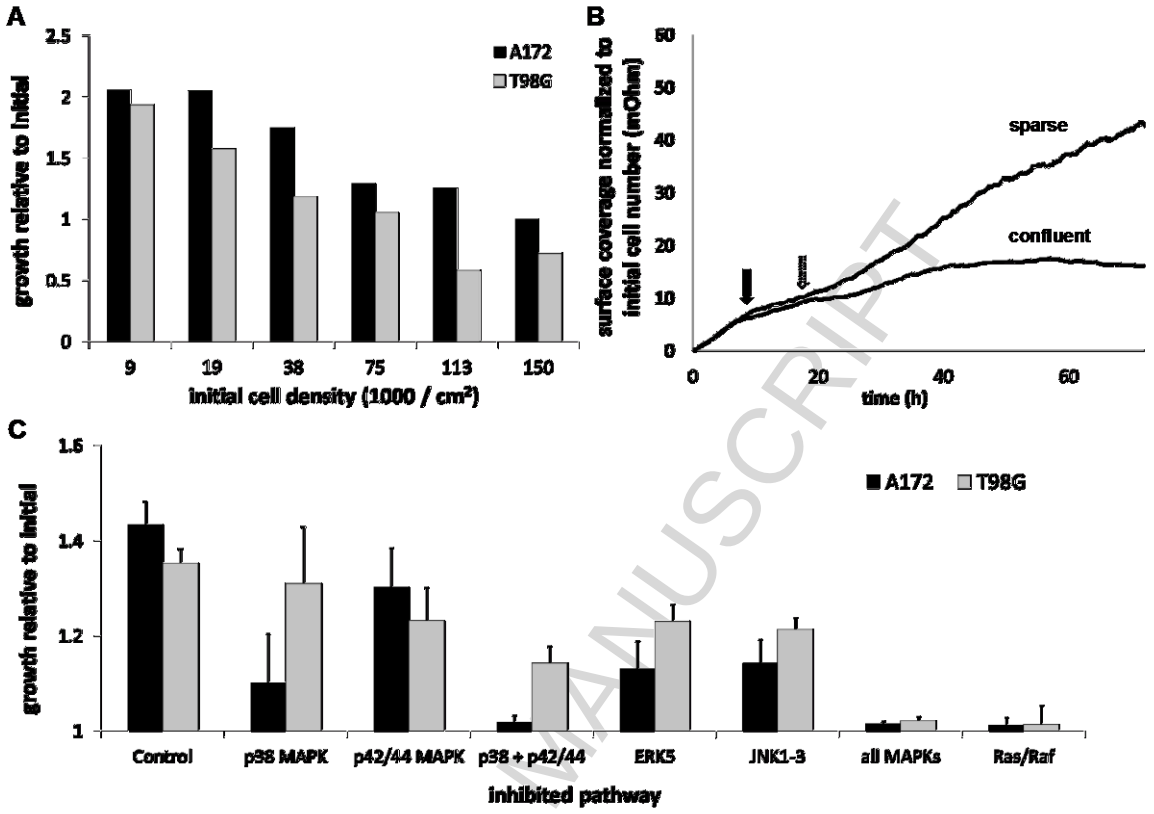

Figure 4

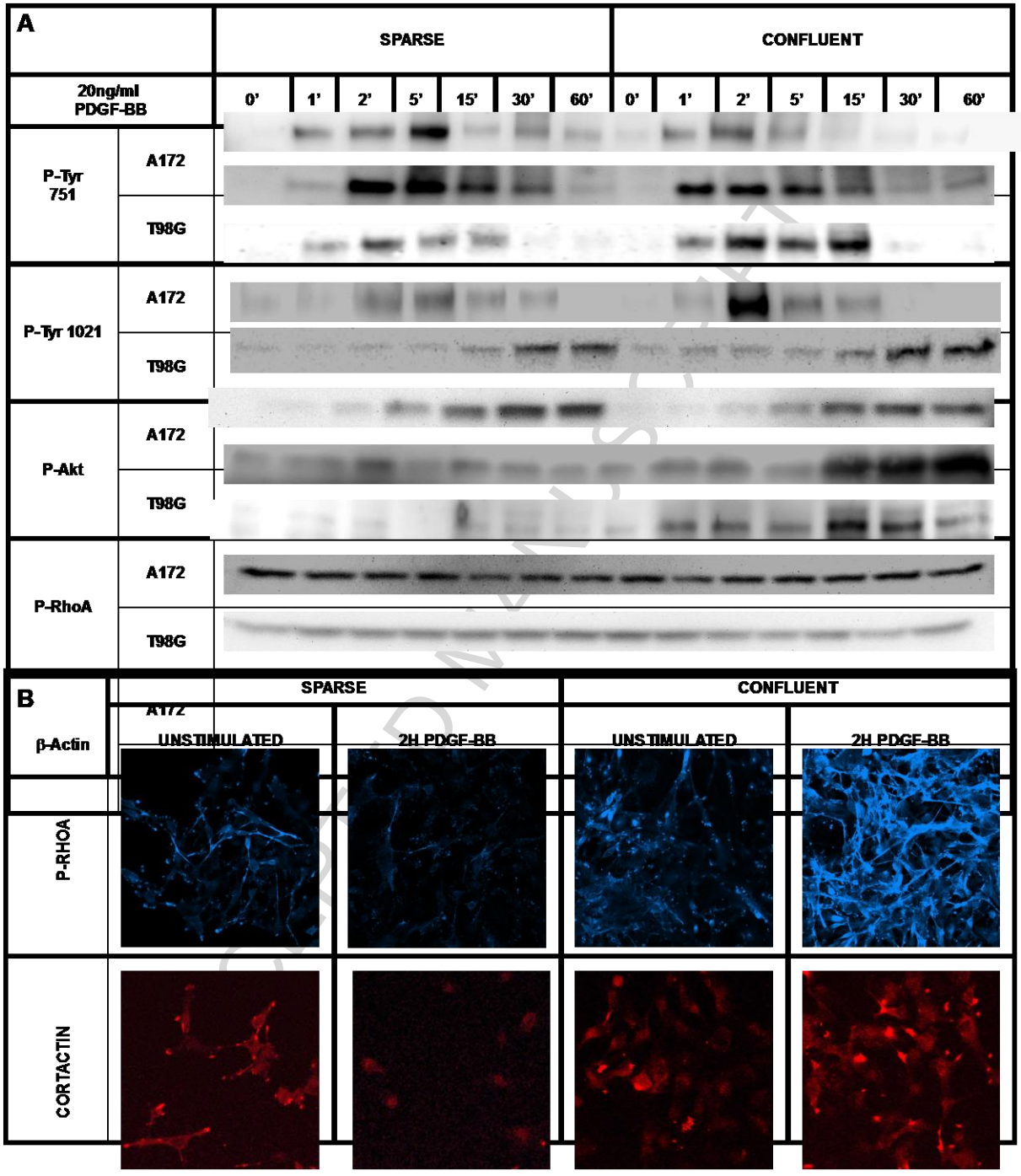

Figure 5

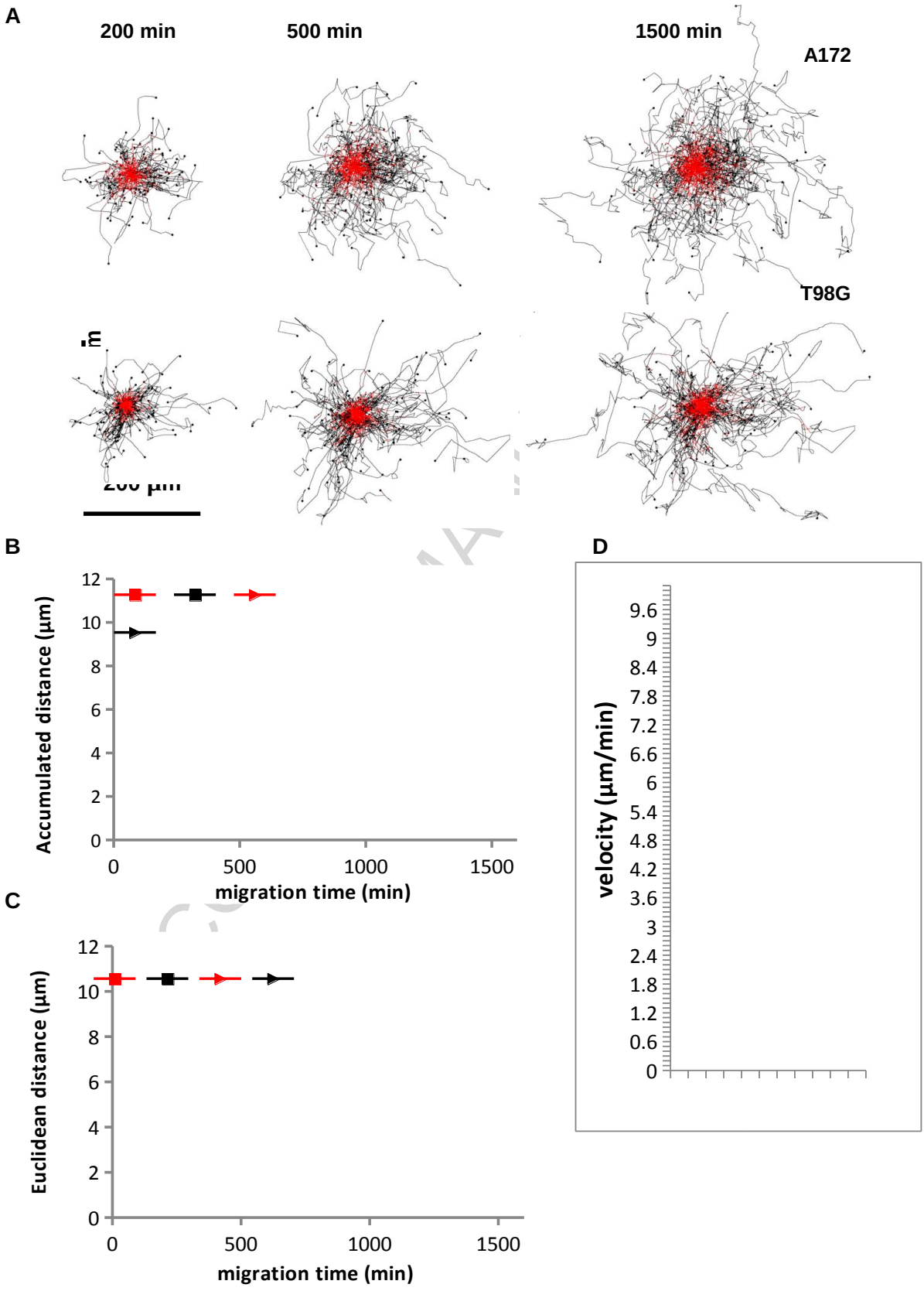

Figure 6

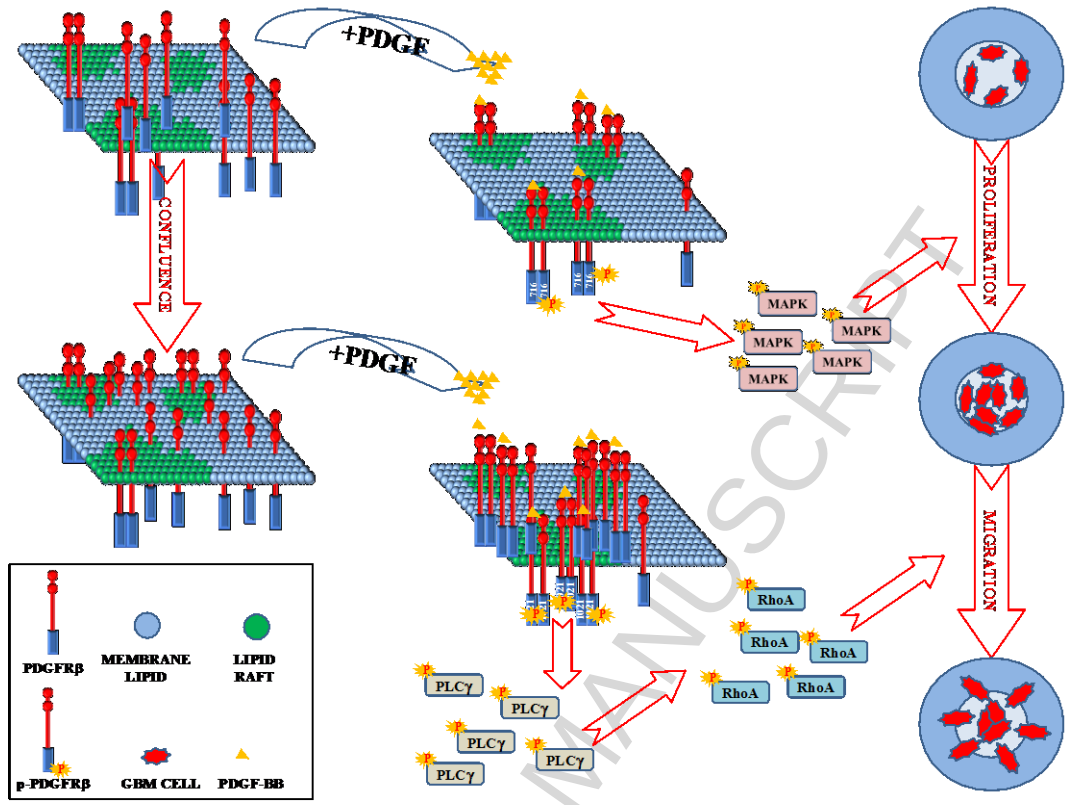

Graphical abstract

Highlights

- PDGFR-β is co-localized with GM1-rich microdomains in the cell membrane and this co-localization increases with cell culture confluence
- Specific tyrosine residues of PDGFR-β are selectively phosphorylated or dephosphorylated as a function of cell confluence, and these processes occur on lipid raft platforms as revealed by quantitative microscopic image analysis
- Activation of the Ras-MAPK pathway and consequential cell proliferation is dominant in sparse cultures
- Activation of the Akt survival kinase shows similar patterns in sparse and confluent cultures
- Activation of the PLCγ pathway, de-activation of the Ras-MAPK pathway and consequential cell migration is dominant in confluent cultures
- Overall, the same stimulus, through a confluence dependent, lipid raft-based regulatory mechanism, is able to promote distinct signaling outputs that are highly relevant to the tumor's actual requirement for proliferation vs. spreading.